Inorganic Chemistry

Article

pubs.acs.org/IC

Probing High-Pressure Phase Transitions in Ti-Based Perovskite-Type Ferroelectrics Using Visible Resonance Raman Spectroscopy

Guillaume Fraysse,*[,†] Jérôme Rouquette,*[,†] Julien Haines,[†] Véronique Bornand,[†] Philippe Papet,[†] and Altaïr Soria Pereira[‡]

[†]Institut Charles Gerhardt Montpellier (ICGM), UMR 5253 CNRS-UM2-ENSCM-UM1, équipe C2M, Université Montpellier II, Place Eugène Bataillon, 34095 Montpellier cedex 5, France

[‡]Instituto de Física e Escola de Engenharia, Universidade Federal do Rio Grande do Sul, 91501-970, Porto Alegre, RS, Brazil.

ABSTRACT: We report unprecedented dramatic changes in the 647.1 nm Raman signal of $PbZr_{0.6}Ti_{0.4}O_3$ occurring in the same pressure ranges as the critical pressures of the antiferrodistortive and ferroelectric-paraelectric phase transitions. This huge decrease in intensity of both the Raman modes and the background, observed for both pressure transmitting media used (glycerol or 4:1 methanol ethanol mixture), is shown to originate from the two-step loss of a resonance Raman effect and the concomitant fluorescence. Changes in the local titanium environment (first with the onset of octahedral tilting and then with the removal of polar cation displacements) alter the electronic band structure and modify the resonance conditions. Furthermore, the optimal resonance conditions are found to be particularly narrow, as shown by the fluorescence spectrum of $PbZr_{0.6}Ti_{0.4}O_3$ at atmospheric pressure characterized by the presence of a very well-defined sharp peak (fwhm = 8 nm) centered around 647.1 nm. These results thus demonstrate that visible resonance Raman spectroscopy can be used as a quick and efficient technique for probing phase transitions in $PbZr_{1-x}Ti_xO_3$ (PZT) and other technologically important perovskite-type materials such as PMN-*x*PT, PZN-*x*PT relaxors, lead free piezoelectrics, and ferroelectric nanopowders. This technique appears also a good alternative to UV Raman spectroscopy for probing the polar order at the nanoscale in ultrathinfilms and superlattices.

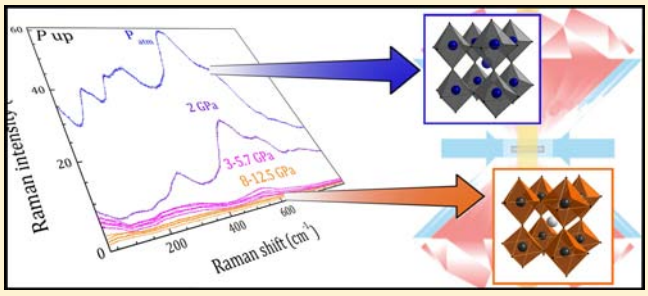

1. INTRODUCTION

Since the 1950s and the pioneering work of Shirane and co-workers,[1−3] the lead zirconate titanate $PbZr_{1-x}Ti_xO_3$ system (PZT) has been the subject of a considerable number of studies mainly triggered by its importance in transducers, actuators, MEMS, and nonvolatile memory applications. However, there remain unsettled issues, notably regarding the composition−temperature (*x*-*T*) phase diagram. The boundaries between the different phases and their symmetry, in particular close to the morphotropic phase boundary (a composition-induced phase transition separating "rhombohedral" from "tetragonal" ferroelectric phases, abbreviated as MPB) are still a subject of intense debate.[4−12] Among the numerous experimental techniques used to elucidate these issues, Raman spectroscopy has been widely applied (Raman scattering being very sensitive to phase transitions because of the different selection rules which change as a function of crystal symmetry).[13,14] This technique has been used in particular to confirm the existence of a monoclinic phase, which was discovered in the MPB using high-resolution synchrotron X-ray diffraction measurements (the transition from tetragonal to monoclinic structure being evidenced by the transformation of the B_1 and E modes into A″ and A′+A″, respectively).[15] Several Raman spectroscopic studies were also performed over larger compositional ranges with the aim of determining the stability range of this low-symmetry phase, but variation of the signal was found to be very subtle.[16,17] With the report of a second monoclinic phase at very low temperature,[18] Raman measurements were also carried out as a function of temperature. The transition from the "high" temperature monoclinic *Cm* to the low temperature monoclinic *Cc* phase, which involves doubling of the unit cell, should cause the appearance of extra modes. However, because of the well-known static and dynamic disorder in the PZT system, only minor spectral changes were observed (conventional Raman spectroscopy measurements providing information on the average structure of the B atom with the associated intrinsic dipole moment).[16,17] The recent discovery of a resonance Raman effect in morphotropic $PbZr_{0.52}Ti_{0.48}O_3$, originating from a self-trapped level exciton energy deficient complex (Ti_{Ti}'-$V_O^{\bullet\bullet}$ with an energy close to the 647.1 nm excitation line,[19] may permit the characterization of such a ferroelectric-ferroelectric phase transition using visible Raman spectroscopy (it should be noted that in PZT the Zr atom is in a disordered pseudocentrosymmetric position and that the dipole moment originates almost solely from the Ti off-center displacement).[20] Rouquette et al. have shown indeed that, in contrast to the spectra obtained with the 514.5 nm excitation

Received: February 20, 2012
Published: November 12, 2012

line where the temperature effect was minor, the Raman signal obtained with the 647.1 nm line exhibits major spectral changes as a function of temperature in close agreement with the antiferrodistortive transition temperature previously determined by other techniques. Corroborating the existence of this resonance Raman effect is of prime importance as one could take advantage of this phenomenon for probing the polar character of the Ti atom and thus accurately determining the critical temperature (pressure) of ferroelectric-paraelectric phase transitions or the onset of octahedral tilting in perovskite-type ferroelectrics using a simple conventional Raman spectrometer, while this usually requires the use of neutron diffraction.

The purpose of this work is thus 3-fold: (1) first of all, to demonstrate that the resonance Raman effect observed in morphotropic $PbZr_{0.52}Ti_{0.48}O_3$ exists for other compositions, (2) to determine how this resonance effect is affected by high-pressure, knowing that the latter can strongly modify the electronic structure of materials, and finally (3) to confirm that the resonance behavior is structure-dependent. To clarify these issues, high-pressure Raman spectroscopy measurements have been performed on the $PbZr_{0.6}Ti_{0.4}O_3$ composition up to 12.5 GPa.

2. EXPERIMENTAL SECTION

$PbZr_{0.6}Ti_{0.4}O_3$ powder was prepared by the conventional solid-state reaction from high-purity (>99.9%) oxides via a two-stage calcination process.[21] A first set of Raman experiments were carried out using the 647.1 nm excitation line from a krypton-ion laser with a Jobin-Yvon T64000 spectrometer equipped with a triple monochromator, an Olympus microscope and a charge coupled device cooled down to 140 K. Measurements were performed both on increasing and decreasing pressure using a membrane-type diamond anvil cell Diacell Helios (DAC) with low fluorescence-type Ia 400 μm-diameter diamond culets and a large angular access (50°) to collect the highest possible amount of scattered light. The sample was loaded along with a ruby crystal as a pressure calibrant and glycerol as a pressure-transmitting medium in the 120 μm-diameter hole of a stainless-steel gasket, which had been preindented to a thickness of 70 μm and drilled by spark eroding using a 100 μm-diameter tungsten wire. The DAC was closed by applying a pressure on the membrane and then was placed using a micrometric displacement table under the Mitutoyo objective (×50) of the microscope. The pressurization of the membrane was performed step by step using a homemade pressure controller. The pressure was estimated based on the shift of the R_1 fluorescence line of the ruby.[22] In this respect, it should be noted that these Raman spectra were collected in nonhydrostatic conditions (the hydrostatic limit of glycerol has been shown to lie around 1.4 GPa from the measurement of diffraction line broadening in a quartz reference crystal).[23] However, the pressure transmitting medium was found to remain relatively soft throughout the experiments and the optical transparency almost unchanged.[24,25] Regarding the depressurization, a 12-h relaxation time has been necessary for the pressure to decrease from 2.3 GPa to atmospheric pressure. Each time a new pressure was reached, the sample was stabilized for 15 min before acquisition. The laser power was kept to a low value (around 1 mW on the sample) to avoid absorption by the sample and associated localized heating. The Raman signal was obtained in the 30−900 cm^{-1} range after a 2 × 3 × 150 s acquisition time.

A second set of Raman experiments were performed afterward using the same spectrometer, excitation line, laser power, and membrane-type diamond anvil cell, but this time with a 4:1 volume ratio methanol ethanol mixture as a pressure transmitting medium. The Raman signal was measured in the 20−950 cm^{-1} range after a 2 × 3 × 150 s acquisition time. The anti-Stokes signal was also collected at each pressure (in the −20 to −420 cm^{-1} range) to check if Raman spectra follow Bose statistics.

The fluorescence spectrum of $PbZr_{0.6}Ti_{0.4}O_3$ was collected at atmospheric pressure using the 473 nm excitation line of a blue diode laser with a Horiba Jobin-Yvon LabRam Aramis equipped with an Olympus microscope and a CCD cooled by a thermoelectric Peltier device. The laser was focused to a ∼7 μm sized spot on the sample. To prevent damage to the latter, the use of a D1 filter was required, and the acquisition time was limited to 4 s.

It should be noted that all Raman spectra reported in this study are as-collected. Neither intensity increment nor normalization has been performed.

3. RESULTS AND DISCUSSION

3.1. Pressure-Induced Antiferrodistortive (*AFD*) Phase Transition. Raman spectra obtained as a function of increasing pressure are illustrated in Figure 1. One can note first that the

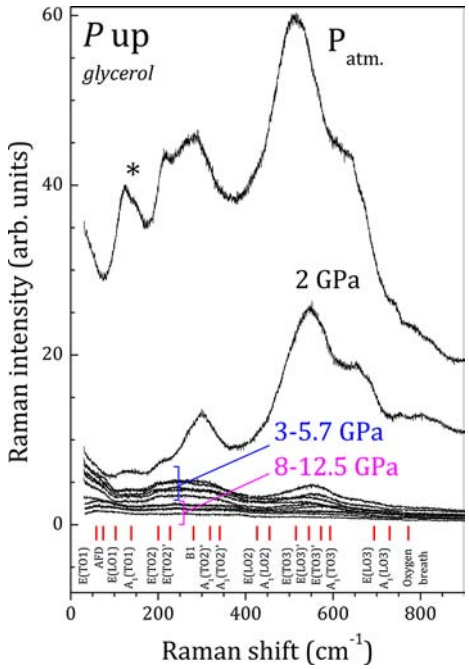

Figure 1. As-collected Raman spectra of $PbZr_{0.6}Ti_{0.4}O_3$ obtained as a function of increasing pressure using glycerol as a pressure transmitting medium. Positions and assignments of Raman modes as reported by Buixaderas et al. for $PbZr_{0.54}Ti_{0.46}O_3$ are shown.[29] The star symbol indicates the position of the polar breathing mode A_1(TO1).

signal collected at atmospheric pressure is still intense at 900 cm^{-1} although no modes are expected in this wavenumber region.[26] There is thus a strong contribution of the background at atmospheric pressure. Furthermore, whereas most of previous studies performed on PZT ceramics have evidenced relative subtle changes in the Raman signal in the course of phase transitions,[15−17,27−29] the present Raman signal evolve drastically as a function of pressure. Raman modes, in particular the polar breathing mode A_1(TO1) centered around 125 cm^{-1}, are found to decrease strongly in intensity between atmospheric pressure and 2 GPa. This huge reduction continues between 2 and 3 GPa for the two broad bands centered at 250 cm^{-1} and 550 cm^{-1}. Besides the dramatic decrease in intensity of the phonons, it seems that the background also decreases significantly from P_{atm} to 3 GPa.

To try to understand the origin of this luminescence background component, the anti-Stokes signal was collected as a first step. As has been reported for the morphotropic composition at atmospheric pressure, Bose-corrected Stokes

dx.doi.org/10.1021/ic300381r | Inorg. Chem. 2012, 51, 12619−12625

intensity was found to be higher than anti-Stokes intensity.[19] Since then, one may conclude that the background contribution originates solely from fluorescence. The fluorescence spectrum collected after decompression at atmospheric pressure (Figure 2) unambiguously confirmed our conclusion. $PbZr_{0.6}Ti_{0.4}O_3$ is

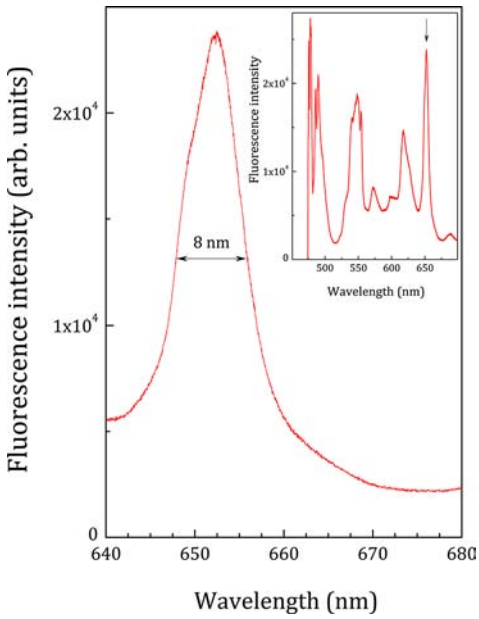

Figure 2. Fluorescence spectrum of $PbZr_{0.6}Ti_{0.4}O_3$ at atmospheric pressure around 647.1 nm (i.e., the excitation line used for the Raman experiments). Inset illustrates the full spectrum.

found indeed to be characterized by a strong fluorescence signal with a very well-defined sharp peak centered around 647.1 nm, that is, the excitation line used for Raman experiments (the full width at half-maximum of this peak being only 8 nm).

The background intensity may be thus estimated by fitting a Gaussian function to the data. The integrated intensity of the Gaussian is found to decrease by more than a factor of 10 between atmospheric pressure and 3 GPa (Figure 3).

Such a huge decrease in intensity of both the Raman modes and the background may be explained by a change in the resonance conditions. As the same excitation line has been used

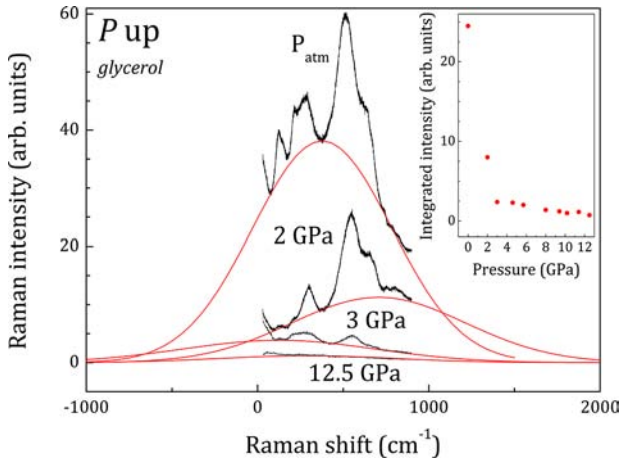

Figure 3. Pressure dependence of the Gaussian function used to fit the background (fluorescence). Inset illustrates the evolution of the Gaussian's integrated intensity.

all along the experiments, the electronic structure is probably involved in this resonance Raman effect. This sudden variation is thus certainly due to a phase transition as the latter will lead to a modification of the local titanium environment resulting in a change in the band structure. As it has been shown recently in a neutron and X-ray powder diffraction study that an antiferrodistortive phase transition occurs in this pressure range,[30] one may reasonably assume that the dramatic decrease of the Raman signal is a consequence of the phase transition. In this way, the modification of the band structure will cause the almost complete disappearance of the resonance Raman effect and the concomitant fluorescence. At higher pressure, the evolution of the Raman signal is found to be less marked. However, one can notice a decrease in intensity of the mode centered at 50 cm^{-1} as well as the broad bands centered at 250 cm^{-1} and at 550 cm^{-1}. A careful analysis is necessary to know if the resonance Raman effect remains beyond 3 GPa or if the Raman signal at high pressure originates solely from the conventional Raman effect. The high-pressure behavior will be discussed in detail later.

Raman spectra obtained as a function of decreasing pressure are illustrated in Figure 4. The Raman signal is found to vary slightly from 12.5 to 2.3 GPa before increasing just as dramatically as the decrease observed through compression.

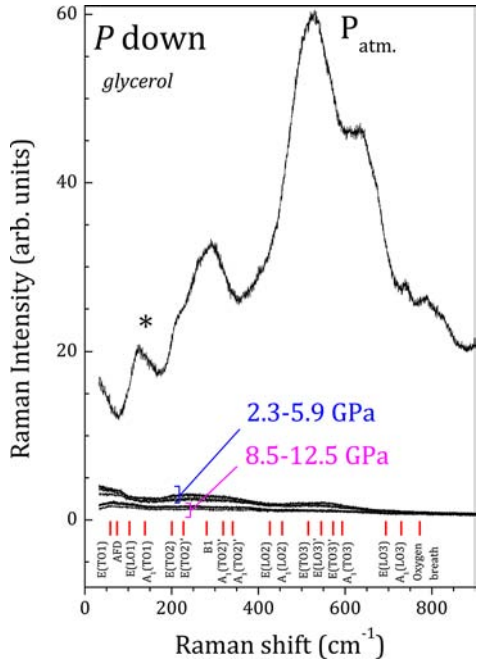

Figure 4. As-collected Raman spectra of $PbZr_{0.6}Ti_{0.4}O_3$ obtained as a function of decreasing pressure using glycerol as a pressure transmitting medium. Positions and assignments of Raman modes as reported by Buixaderas et al. for $PbZr_{0.54}Ti_{0.46}O_3$ are shown.[29] The star symbol indicates the position of the polar breathing mode A_1(TO1).

This sudden increase in intensity of both the modes and the background between 2.3 GPa and atmospheric pressure indicates the reappearance of the resonance Raman effect and the fluorescence (Figure 5). As this phenomenon appears to be reversible, it confirms our assumption according to which the modification of the band structure in the course of the antiferrodistortive phase transition leads to a change in the resonance conditions. Interestingly, the Raman spectrum at atmospheric pressure differs to a slight extent from that

dx.doi.org/10.1021/ic300381r | Inorg. Chem. 2012, 51, 12619−12625

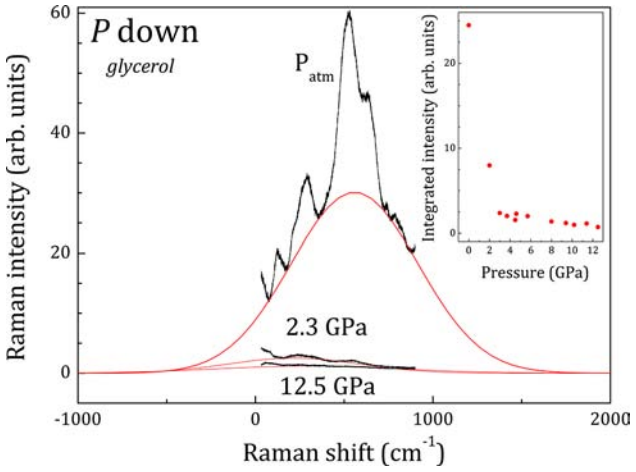

Figure 5. Pressure dependence of the Gaussian function used to fit the background (fluorescence). Inset illustrates the evolution of the Gaussian's integrated intensity.

obtained before compression. In particular, the background contribution seems to be noticeably weaker at low frequencies. Looking at the insets of Figure 3 and Figure 5, one can note that the integrated intensities of the Gaussian show almost exactly the same trends and values. The Gaussian fit is actually shifted to higher frequencies thus resulting in a lower background at lower frequencies. This is consistent with the very diffuse nature of the pressure-induced *AFD* phase transition.[30] Indeed, as the phase ratio between the untilted and the tilted ferroelectric phases is different before and after compression because of the nature of the transition, the position of the fluorescence signal is expected to have changed and consequently the center of the Gaussian function.

3.2. Pressure-Induced Ferroelectric-Paraelectric (*FE-PE*) Phase Transition. Let us now focus on the high-pressure behavior of the Raman signal. Although the evolution of Raman spectra beyond 3 GPa is with no possible comparison as significant as that observed at lower pressure, one can notice some changes that could be linked to the pressure-induced ferroelectric-paraelectric phase transition. The polar breathing mode $A_1(TO1)$ is actually still present at 3 GPa even if its intensity is relatively weak (Figure 6A). The intensity of this mode continues to decrease upon compression until vanishing between 5.7 and 8 GPa. Concurrently, the mode at 50 cm^{-1} and the broad bands centered around 250 cm^{-1} and 550 cm^{-1} weaken noticeably and shift to higher frequencies. No significant evolution of the Raman signal is observed at higher pressure.

Regarding the evolution of the Raman signal upon decompression, spectra collected at 10.5, 9.7, and 8.5 GPa are found to be perfectly superimposed (Figure 6B). Then, an obvious increase of both the background and the Raman modes as well as a shift of the latter to lower frequencies occurs between 8.5 and 5.9 GPa (see inset of Figure 6B). This increase which is probably due to the reappearance of the fluorescence indicates a further change in the resonance conditions. Interestingly, this occurs in the same pressure range as the critical pressure of the ferroelectric-paraelectric phase transition determined previously using neutron and X-ray powder diffraction.[30] Once again it is reasonable to think that this sudden increase is due to the *FE-PE* phase transition. Therefore, the modification of the band structure upon

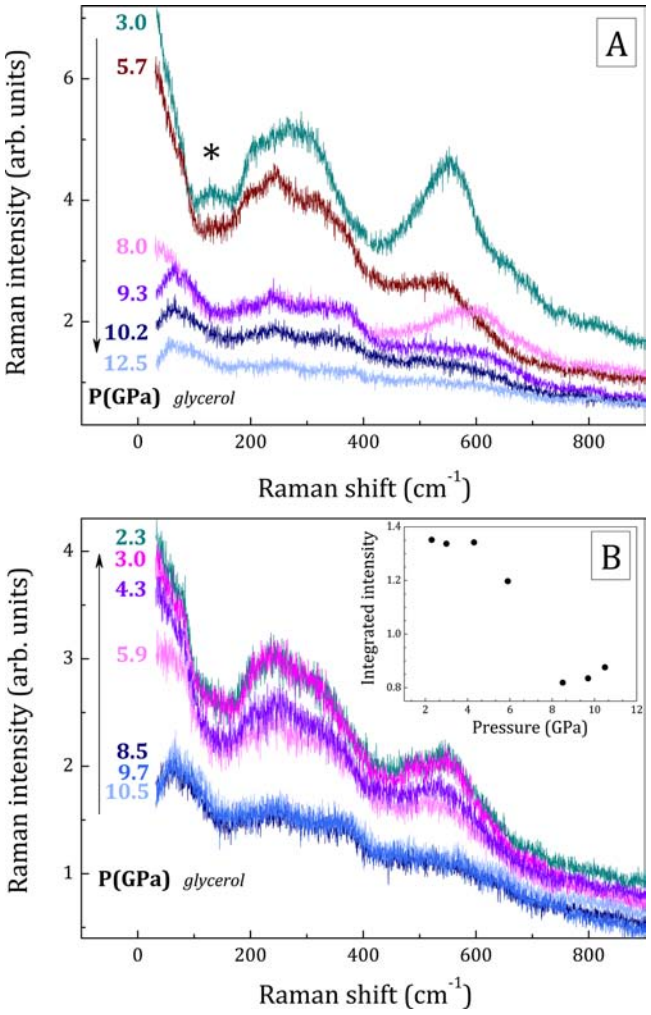

Figure 6. Selected 647.1 nm Raman spectra illustrating the disappearance and reappearance of polar order in $PbZr_{0.6}Ti_{0.4}O_3$ with increasing (A) and decreasing (B) pressure respectively (with glycerol as a pressure transmitting medium). Several spectra obtained upon compression were not reported for clarity. The pressure dependence of the Gaussian's integrated intensity is shown in the inset.

decreasing pressure (first with the onset of polar cation displacements and then with the removal of octahedral tilting) could narrow the gap with optimal resonance Raman conditions after having shifted upon compression.

3.3. Pressure Dependence of the Resonance Raman Effect under Hydrostatic Conditions. To remove any doubt on the origin of the huge Raman intensity decreases/enhancements, a second set of experiments was performed using a 4:1 volume ratio methanol ethanol mixture known to be perfectly hydrostatic up to 9.8 GPa.[23] As-collected Raman spectra obtained using this pressure transmitting medium are reported in Figure 7. Once again, one can observe an important decrease in intensity of both the Raman modes and the background in the course of the pressure-induced antiferrodistortive phase transition (i.e., from atmospheric pressure to ~2 GPa).[30] This is not the result of changes in the optical transparency of the pressure transmitting medium and is strong evidence of the phase transition (the small differences between the two experiments may be due to the position of the fluorescence signal and to the very diffuse nature of the

dx.doi.org/10.1021/ic300381r | *Inorg. Chem.* 2012, 51, 12619–12625

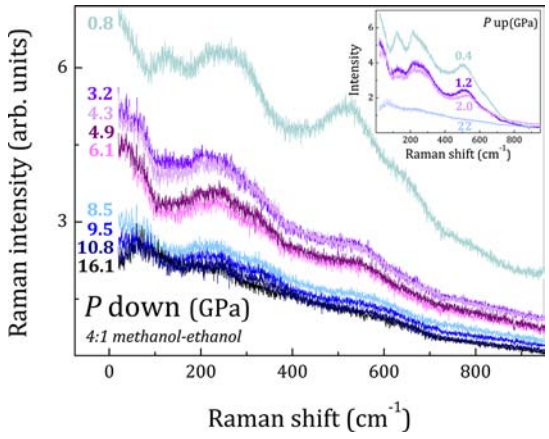

Figure 7. As-collected Raman spectra of $PbZr_{0.6}Ti_{0.4}O_3$ obtained as a function of decreasing pressure using a 4:1 volume ratio methanol ethanol mixture as a pressure transmitting medium. Inset illustrates selected Raman spectra obtained as a function of increasing pressure.

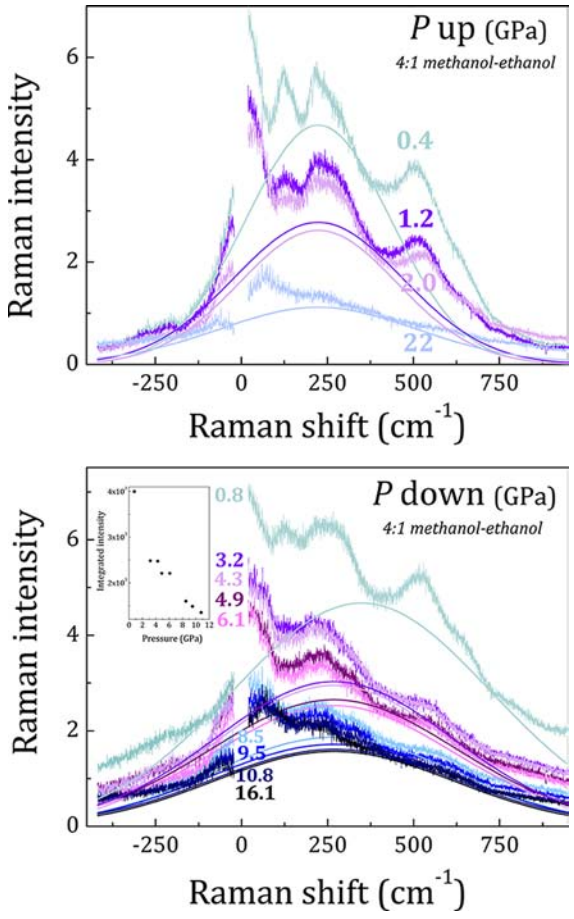

Figure 8. Evolution of the Stokes-anti-Stokes Raman spectrum of $PbZr_{0.6}Ti_{0.4}O_3$ as a function of increasing (A) and decreasing pressure (B) illustrating the important decrease/enhancement of the fluorescence signal. The pressure dependence of the integrated intensity of the Gaussian is shown in the inset.

antiferrodistortive phase transition).[30] As has been observed previously using glycerol, a second decrease of the luminescence background and the Raman modes also occurs between 8.5 and 6.1 GPa (i.e., in the pressure range of the paraelectric-ferroelectric phase transition). These results thus confirm that the spectacular changes observed previously in the Raman signal were not due to the loss of hydrostaticity of glycerol and do result from changes in the local environment of titanium.

To follow carefully the pressure dependence of the resonance Raman effect and the concomitant fluorescence, the anti-Stokes signal has been collected at each pressure, Figure 8. The luminescence background contribution (i.e., the fluorescence), which can be described by a Gaussian irrespective of the pressure, shifts significantly to higher frequencies upon decreasing pressure, thereby explaining the mismatch observed at moderate pressure between spectra collected upon increasing and decreasing pressure. This is consistent once again with the very diffuse nature of the pressure induced antiferrodistortive phase transition.[30] It should also be noted that the difference between Bose-corrected Stokes and anti-Stokes intensities, which is direct evidence of the existence of the resonance Raman effect,[19] decreases upon compression and then increases upon decompression. Raman experiments performed under hydrostatic conditions (i.e., using a 4:1 volume ratio methanol ethanol mixture) have thus led to exactly the same conclusions than experiments performed using glycerol as a pressure transmitting medium.

3.4. Probing Phase Transitions in Ti-Based Perovskites Using Visible Resonance Raman Spectroscopy. The evolution of the Raman signal of $PbZr_{0.6}Ti_{0.4}O_3$ as a function of pressure is shown to be characterized by two huge and reversible changes in intensity. The first one occurs at "moderate" pressure in the same pressure range as the critical pressure of the antiferrodistortive phase transition previously determined by X-ray and neutron diffraction. The second one coincides with the disappearance of the polar breathing mode $A_1(TO1)$ and thus with the occurrence of the ferroelectric-paraelectric phase transition. Furthermore, contrary to what has been reported, for instance, for boron carbide[31] or for single-wall carbon nanotubes when the resonance occurs with the scattered photon[32,33] these Raman intensity decreases/enhancements do not concern only one particularly mode or family of modes with the same symmetry but the entire signal making the *AFD* and *FE-PE* phase transitions identifiable at a glance. It is also found that the exciton level and consequently the optimal resonance conditions are particularly narrow at atmospheric pressure (see Figure 2). Thus, any change in pressure will result in a modification of the intensity of both the Raman modes and the background. Interestingly, these changes will be much greater more important at a pressure-induced phase transition. Raman spectroscopy measurements with the 647.1 nm excitation line appears thus a simple and fast technique for probing phase transitions in the PZT system and should help to solve controversial aspects of the phase diagram. In particular, measurements on tetragonal compositions near the MPB may provide new insight in the antiferrodistortive phase transition predicted by first principle calculations[4] and observed experimentally by anelastic spectroscopy measurements.[5] Indeed, although recent conventional Raman spectroscopy measurements have permitted the existence of the tetragonal tilted phase to be confirmed (the transition from the low to the high-temperature tetragonal phase being marked by the splitting of the $E+B_1$ mode),[28] changes in the Raman signal were very subtle and no precise critical temperature could be measured. This technique should also be very useful to corroborate the existence of the phase transition recently reported near the antiferroelectric-ferroelectric phase boundary

dx.doi.org/10.1021/ic300381r | *Inorg. Chem.* 2012, 51, 12619−12625

for temperatures above the tilt boundary.[11] Indeed, if this new diffuse transition consists, as it was proposed by Cordero et al., in the onset of disordered tilting of BX_6 octahedra before the long-range ordered tilt pattern develops at the well-established tilt boundary, the resonance Raman signal should evolve significantly between the two critical temperatures because of changes in the local titanium environment.

This resonance Raman effect is also very likely to exist in other Ti-based perovskites as it has been shown that they display similar visible photoluminescence between 2 and 3 eV.[34,35] Thus, one could take advantage of this phenomenon for clarifying the phase diagram of the technologically important relaxor ferroelectric $PbMg_{1/3}Nb_{2/3}O_3$-$x$$PbTiO_3$ (PMN-xPT) and $PbZn_{1/3}Nb_{2/3}O_3$-$x$$PbTiO_3$ (PZN-xPT) compounds, which also exhibit significant static and dynamic disorder. Conventional Raman spectra of these materials generally consist of broad lines that are not well resolved and do not change drastically as a function of temperature, pressure, or composition.[36−41]

Visible resonance Raman spectroscopy could be also very useful for investigating lead-free piezoelectric materials (such as those belonging to $BaTiO_3$, $Bi_{1/2}Na_{1/2}TiO_3$, $Bi_{1/2}K_{1/2}TiO_3$−based systems) as well as ferroelectric nanopowders. Probing polar order in the former may be complicated indeed by the fact that the crystal structure of the ferroelectric phase is often close to cubic. For instance, neutron and high-resolution X-ray diffraction measurements performed on different compositions of the promising (1-x-y)BNT-xBT-yKNN system have indicated a long-range-ordered pseudocubic lattice while the polarization field curves pointed to perfectly ferroelectric materials.[42,43] Determining the critical temperature of the ferroelectric paraelectric phase transition in nanopowders is also not obvious. In such materials, the differences between X-ray diffraction patterns of ferroelectric and paraelectric phases only consist in asymmetric broadening of the cubic reflections (the critical temperature being estimated by following the full width at half-maximum of the different reflections).[44]

It is also well-known that probing the polar order in ultrathin films and superstructures using conventional visible Raman spectroscopy works poorly because of overwhelming signals generated when the light travels through the film into the substrate (the low energy of the excitation line in comparison with the band gap leading to extremely weak absorption and thus large penetration depth). This has incited researchers to use UV excitation lines (the photon energy being in this case larger than the band gaps of ferroelectrics). If, at first, researchers came up against the lower throughput efficiency and the higher stray light level of UV Raman spectrometers as compared to those operating in the visible range, recent progress in UV Raman instrumentation have made this measurement possible. Using powerful laser sources and optimized optical paths, Tenne et al. have indeed succeed in measuring the T_C of the $BaTiO_3$ layers in 24 nm thick $BaTiO_3$/$SrTiO_3$ superlattices.[45] Nevertheless, such a UV Raman spectroscopy setup is not easily available. In the present study, we have shown that the polar as well as the antiferrodistortive order can be probed in PZT ceramics without any difficulty using a conventional spectrometer. Thus, even if the visible resonance Raman spectroscopy does not provide the same information as UV Raman spectroscopy as electronic transitions involved in these techniques are different, it could be a good alternative to the latter for probing ferroelectricity at the nanoscale in ultrathinfilms and superlattices.

4. CONCLUSION

We have reported a high-pressure visible Raman spectroscopy study of $PbZr_{0.6}Ti_{0.4}O_3$ ceramics in which we succeed in probing antiferrodistortive and polar orders in spite of their well-known static and dynamic disorder, taking advantage of the resonance Raman effect recently discovered in morphotropic composition.[19] The antiferrodistortive and ferroelectric-paraelectric phase transitions previously evidenced by neutron and X-ray powder diffraction measurements[30] have been revealed by two dramatic reversible changes in the Raman signal obtained using the 647.1 nm excitation line. These huge decreases/increases, which, to the best of our knowledge have no precedent among reported Raman studies on solid state materials, are shown to originate from the modification of the band structure in the course of pressure-induced phase transitions. As the resonance behavior is shown to be structure dependent and the optimal resonance conditions particularly narrow, one could take advantage of this phenomenon to probe phase transitions in the technologically important PZT system. These results have great implications in materials sciences as this resonance Raman effect is very likely to exist in other Ti-based perovskite compounds.

We hope that this study will stimulate further research on this resonance Raman effect and the concomitant fluorescence. Investigations under the best conditions possible, namely, at atmospheric pressure and using single crystals of PZT, are particularly encouraged to resolve some relevant points, which remain unsettled, such as the nature of the photon involved in this resonance effect (incident or scattered), and the selection rules.

AUTHOR INFORMATION

Corresponding Author

*E-mail: Guillaume.Fraysse@univ-montp2.fr (G.F.), Jerome.Rouquette@univ-montp2.fr (J.R.).

Notes

The authors declare no competing financial interest.

ACKNOWLEDGMENTS

We gratefully acknowledge Dr. Jean-Louis Sauvajol and David Maurin (Laboratoire Charles Coulomb, Université Montpellier II) for the use of the Jobin-Yvon T64000 Raman spectrometer, David Bourgogne (ICGM) for technical assistance with the LabRam Aramis spectrometer, and Dr. A. Al-Zein (SPMS, École Centrale Paris) for fruitful discussions.

REFERENCES

(1) Shirane, G.; Takeda, A. *J. Phys. Soc. Jpn.* **1952**, *7*, 5.
(2) Shirane, G.; Suzuki, K.; Takeda, A. *J. Phys. Soc. Jpn.* **1952**, *7*, 12.
(3) Shirane, G.; Suzuki, K. *J. Phys. Soc. Jpn.* **1952**, *7*, 333.
(4) Kornev, I. A.; Bellaiche, L.; Janolin, P.-E.; Dkhil, B.; Suard, E. *Phys. Rev. Lett.* **2006**, *97*, 157601.
(5) Cordero, F.; Craciun, F.; Galassi, C. *Phys. Rev. Lett.* **2007**, *98*, 255701.
(6) Fraysse, G.; Haines, J.; Bornand, V.; Rouquette, J.; Pintard, M.; Papet, Ph.; Hull, S. *Phys. Rev. B* **2008**, *77*, 064109.
(7) Pandey, D.; Singh, A. K.; Baik, S. *Acta Crystallogr., Sect. A* **2008**, *64*, 192−203.
(8) Yokota, H.; Zhang, N.; Taylor, A. E.; Thomas, P. A.; Glazer, A. M. *Phys. Rev. B* **2009**, *80*, 104109.

(9) Phelan, D.; Long, X.; Xie, Y.; Ye, Z.-G.; Glazer, A. M.; Yokota, H.; Thomas, P. A.; Gerhing, P. M. *Phys. Rev. Lett.* **2010**, *105*, 207601.
(10) Gorfman, S.; Keeble, D. S.; Glazer, A. M.; Long, X.; Xie, Y.; Ye, Z.-G.; Collins, S.; Thomas, P. A. *Phys. Rev. B* **2011**, *84*, 020102(R).
(11) Cordero, F.; Trequattrini, F.; Craciun, F.; Galassi, C. *J. Phys.: Condens. Matter* **2011**, *23*, 415901.
(12) Zhang, N.; Yokota, H.; Glazer, A. M.; Thomas, P. A. *Acta Crystallogr., Sect. B* **2011**, *67*, 386−398.
(13) Weber, W. H.; Merlin, R. *Raman scattering in materials science*; Springer: Berlin, Germany, 2000.
(14) Haines, J.; Rouquette, J.; Bornand, V.; Pintard, M.; Papet, Ph.; Gorelli, F. A. *J. Raman Spectrosc.* **2003**, *34*, 519−523.
(15) Souza Filho, A. G.; Lima, K. C. V.; Ayala, A. P.; Guedes, I.; Freire, P. T. C.; Mendes Filho, J.; Araujo, E. B.; Eiras, J. A. *Phys. Rev. B* **2000**, *61*, 14283−14286.
(16) Lima, K. C.; Souza Filho, A. G.; Ayala, A. P.; Mendes Filho, J.; Freire, P. T. C.; Melo, F. E. A.; Araujo, E. B.; Eiras, J. A. *Phys. Rev. B* **2001**, *63*, 184105.
(17) Souza Filho, A. G.; Lima, K. C.; Ayala, A. P.; Guedes, I.; Freire, P. T. C.; Melo, F. E. A.; Mendes Filho, J.; Araujo, E. B.; Eiras, J. A. *Phys. Rev. B* **2002**, *66*, 132107.
(18) Hatch, D. M.; Stokes, H. T.; Ranjan, R.; Ragini; Mishra, S. K.; Pandey, D.; Kennedy, B. J. *Phys. Rev. B* **2002**, *65*, 212101.
(19) Rouquette, J.; Haines, J.; Bornand, V.; Pintard, M.; Papet, Ph.; Sauvajol, J. L. *Phys. Rev. B* **2006**, *73*, 224118.
(20) Al-Zein, A.; Fraysse, G.; Rouquette, J.; Papet, Ph.; Haines, J.; Hehlen, B.; Levelut, C.; Aquilanti, G.; Joly, Y. *Phys. Rev. B* **2010**, *81*, 174110.
(21) Rouquette, J.; Haines, J.; Bornand, V.; Pintard, M.; Papet, Ph.; Astier, R.; Léger, J. M.; Gorelli, F. *Phys. Rev. B* **2002**, *65*, 214102.
(22) Sherman, W. F.; Wilkinson, G. R. *Advances in Raman and Infrared Spectroscopy*; Clark, R. J. H., Hester, R. E., Eds.; Heyden: London, U.K., 1980; Vol. *6*, p 158.
(23) Angel, R. J.; Bujak, M.; Zhao, J.; Gatta, G. D.; Jacobsen, S. D. *J. Appl. Crystallogr.* **2007**, *40*, 26.
(24) As reported by Hensel-Bielowka et al. and Pronin et al. the fragility of glycerol increases by about 35% from atmospheric pressure to 2 GPa but remains almost unchanged at higher pressure. Concurrently, the maximum of the imaginary component of the dielectric permittivity, which is proportional to the optical absorption, does not vary noticeably from atmospheric pressure to 3.4 GPa and then tends to decrease at higher pressure. Hensel-Bielowka, S.; Pawlus, S.; Roland, C. M.; Ziolo, J.; Paluch, M. *Phys. Rev. B* **2004**, *69*, 050501. Pronin, A. A.; Kondrin, M. V.; Lyapin, A. G.; Brazhkin, V. V.; Volkov, A. A.; Lunkenheimer, P.; Loidl, A. *Phys. Rev. B* **2010**, *81*, 041503.
(25) The only drawback in using glycerol as a pressure transmitting medium consists in an increase of the full width at half-maximum of the phonons (mainly in the course of the liquid-glass transition). As the latter are already broad at atmospheric pressure, it cannot explain the reported dramatic changes in intensity of both the Raman modes and the background.
(26) Burns, G.; Scott, B. A. *Phys. Rev. Lett.* **1970**, *25*, 1191−1194.
(27) Souza Filho, A. G.; Faria, J. L. B.; Freire, P. T. C.; Ayala, A. P.; Sasaki, J. M.; Melo, F. E. A.; Mendes Filho, J.; Araujo, E. B.; Eiras, J. A. *J. Phys.: Condens. Matter* **2001**, *13*, 7305−7314.
(28) Deluca, M.; Fukumura, H.; Tonari, N.; Capiani, C.; Hasuike, N.; Kisoda, K.; Galassi, C.; Harima, H. *J. Raman Spectrosc.* **2011**, *42*, 488−495.
(29) Buixaderas, E.; Berta, M.; Kozielski, L.; Gregora, I. *Phase Transitions* **2011**, *84*, 528.
(30) Fraysse, G.; Al-Zein, A.; Haines, J.; Rouquette, J.; Bornand, V.; Papet, Ph.; Bogicevic, C.; Hull, S. *Phys. Rev. B* **2011**, *84*, 144110.
(31) Guo, J.; Zhang, L.; Fujita, T.; Goto, T.; Chen, M. *Phys. Rev. B* **2010**, *81*, 060102(R).
(32) Souza Filho, A. G.; Jorio, A.; Hafner, J. H.; Lieber, C. M.; Saito, R.; Pimenta, M. A.; Dresselhaus, G.; Dresselhaus, M. S. *Phys. Rev. B* **2001**, *63*, 241404(R).
(33) Merlen, A.; Bendiab, N.; Toulemonde, P.; Aouizerat, A.; San Miguel, A.; Sauvajol, J. L.; Montagnac, G.; Cardon, H.; Petit, P. *Phys. Rev. B* **2005**, *72*, 035409.
(34) Eglitis, R. I.; Kotomin, E. A.; Borstel, G. *J. Phys.: Condens. Matter* **2002**, *14*, 3735−3741.
(35) Mochizuki, S. S.; Fujishiro, F.; Minami, S. *J. Phys.: Condens. Matter* **2005**, *17*, 923−948.
(36) Ahart, M.; Cohen, R. E.; Struzhkin, V.; Gregoryanz, E.; Rytz, D.; Prosandeev, S. A.; Mao, H.; Hemley, R. J. *Phys. Rev. B* **2005**, *71*, 144102.
(37) El Marssi, M.; Dammak, H. *Solid State Commun.* **2007**, *142*, 487−491.
(38) Slodczyk, A.; Kania, A.; Daniel, Ph.; Ratuszna, A. *J. Phys. D: Appl. Phys.* **2005**, *38*, 2910−2918.
(39) Slodczyk, A.; Daniel, Ph.; Kania, A. *Phys. Rev. B* **2008**, *77*, 184114.
(40) Chaabane, B.; Kreisel, J.; Bouvier, P.; Lucazeau, G.; Dkhil, B. *Phys. Rev. B* **2004**, *70*, 134114.
(41) Kamba, S.; Buixaderas, E.; Petzelt, J.; Fouset, J.; Nosek, J.; Bridenbaugh, P. *J. Appl. Phys.* **2003**, *93*, 933−939.
(42) Hinterstein, M.; Knapp, M.; Hölzel, M.; Jo, W.; Cervellino, A.; Ehrenberg, H.; Fuess, H. *J. Appl. Crystallogr.* **2010**, *43*, 1314−1321.
(43) Zhang, S.-T.; Kounga, A. B.; Aulbach, E.; Granzow, T.; Jo, W.; Kleebe, H.-J.; Rödel, J. *Appl. Phys.* **2008**, *103*, 034107.
(44) Alilat, K.; Pham Thi, M.; Dammak, H.; Bogicevic, C.; Albareda, A.; Doisy, M. *J. Eur. Ceram. Soc.* **2010**, *30*, 1919−1924.
(45) Tenne, D. A.; Bruchhausen, A.; Lanzillotti-Kimura, N. D.; Fainstein, A.; Katiyar, R. S.; Cantarero, A.; Soukiassian, A.; Vaithyanathan, V.; Haeni, J. H.; Tian, W.; Schlom, D. G.; Choi, K. J.; Kim, D. M.; Eom, C. B.; Sun, H. P.; Pan, X. Q.; Li, Y. L.; Chen, L. Q.; Jia, Q. X.; Nakhmanson, S. M.; Rabe, K. M.; Xi, X. X. *Science* **2006**, *313*, 1614−1616.